



Phytolith-rich layers from the Late Bronze and Iron Ages at Tel Dor (Israel): mode of formation and archaeological significance

Rosa Maria Albert ^{a,*}, Ruth Shahack-Gross ^{b,h}, Dan Cabanes ^c, Ayelet Gilboa ^d,
Simcha Lev-Yadun ^e, Marta Portillo ^a, Ilan Sharon ^f, Elisabetta Boaretto ^{b,h}, Steve Weiner ^g

^a Catalan Institution for Research and Advanced Studies (ICREA)/Research Group for Palaeoecological and Geoarchaeological Studies, Department of Prehistory, Ancient History and Archaeology, Universitat de Barcelona, c/ Montalegre, 6-8. 08001 Barcelona, Spain

^b Kimmel Center for Archaeological Science, Weizmann Institute of Science, Rehovot 76100, Israel

^c Àrea de Prehistòria, Depart. Geografia i Història, Universitat Rovira i Virgili/IPHES, Plaça Imperial Tàrraco no. 1, 43005 Tarragona, Spain

^d Zinman Institute of Archaeology, University of Haifa, Mount Carmel, Haifa 31905, Israel

^e Department of Biology, University of Haifa – Oranim, Tivon 36006, Israel

^f Institute of Archaeology, The Hebrew University of Jerusalem, Mount Scopus, Jerusalem 91905, Israel

^g Department of Structural Biology and the Kimmel Center for Archaeological Science, Weizmann Institute of Science, Rehovot 76100, Israel

^h Department Land of Israel Studies and Archaeology, Bar Ilan University, 52900 Ramat Gan, Israel

Received 8 November 2006; received in revised form 26 January 2007; accepted 25 February 2007

Abstract

The presence of many phytolith-rich layers in late Bronze and Iron Age deposits at Tel Dor, Israel, are indicative of specific locations where plants were concentrated. Detailed studies of six of these phytolith-rich layers and associated sediments from Tel Dor show that the phytoliths were derived mainly from wild and domestic grasses. The most common domestic grass was the cereal *Triticum aestivum* (bread wheat). Three of these layers have a microlaminated microstructure, associated dung spherulites and phosphate nodules; characteristics that all point to the phytolith-rich layers having formed from dung in animal enclosures. In two of the layers, the microlaminated structure is absent while dung spherulites and phosphate nodules are present, suggesting that these too originate from dung that was not deposited in an enclosure. The sixth layer is microlaminated but does not contain spherulites. We thus cannot suggest a parsimonious explanation of its observed properties. Concentrations of burnt phytoliths are present in three locations, implying that dung was either burnt *in situ* or the ashes from burnt dung were re-deposited. The transformation of dung accumulations into phytolith-rich layers involves a loss of organic material and hence a significant reduction in sediment volume, which is clearly apparent in the stratigraphy of some of the locations examined. The volume reduction can be observed in the macrostratigraphy and has important implications with regard to macrostratigraphic interpretation. The presence of abundant phytolith-rich layers on the *tell* has significant implications for the concept of ‘urbanism’ during these periods.

© 2007 Elsevier Ltd. All rights reserved.

Keywords: Phytoliths; Mineralogy; Dung spherulites; Cereals; Micromorphology; Tel Dor; Iron Age; Urbanism

1. Introduction

A systematic study of the sediments from the Late Bronze and Iron Age periods at Tel Dor (Israel) revealed the presence of numerous white layers, whose major component is opaline (siliceous) phytoliths. These layers vary in thickness from millimeters to 30 or so centimeters. They can extend laterally for meters. Shahack-Gross et al. (2005) studied two of these phytolith-rich layers that accumulated within a monumental

* Corresponding author. Catalan Institution for Research and Advanced Studies (ICREA)/Research Group for Palaeoecological and Geoarchaeological Studies, Department of Prehistory, Ancient History and Archaeology, Universitat de Barcelona, c/ Montalegre, 6-8. 08001 Barcelona, Spain. Tel.: +34 934037525; fax: +34 934037541.

E-mail address: rosamaria.albert@icrea.es (R.M. Albert).

¹ Visiting Scientist at the Weizmann Institute of Science.

building of the early Iron Age above the southern harbor. They cover the entire space investigated (part of either a room or an open courtyard) and vary in thickness from a centimeter or so to about 10 cm. Prior to this study, these layers were thought to be lime-plaster floors. Micromorphological and phytolith analysis showed that they are composed almost entirely of phytoliths from grasses. The sediment microstructure revealed a wavy lamination, indicative of trampling. Calcitic spherulites were also present. These are derived from the digestive tracts of ruminants, including common domestic animals such as goats, sheep and cows (Brochier et al., 1992; Canti, 1997, 1998, 1999). Shahack-Gross et al. (2005) concluded that this space was used at some point in time in the early Iron Age as an animal enclosure. The aim of this study is to compare and contrast six different phytolith-rich layers at Tel Dor in order to better understand the manner in which they formed, their implications to site formation processes and their significance to the archaeology of the site.

As phytoliths do not accumulate as such, but are always deposited together with the associated plant organic material, the presence of these layers raises interesting taphonomic questions. Shahack-Gross et al. (2005) reported that the volume proportions of phytoliths to whole modern dung is about 1:50. The reduction in volume that occurs when the organic matter is degraded is considerable. This compression of *tell* sediment over time, can clearly influence the stratigraphy, can concentrate artifacts into smaller volumes and can juxtapose sediment layers against walls that are lower (i.e. older) than the sediments.

It is reasonable to assume that almost all phytoliths were brought to the *tell* while still an integral part of the plants in which they formed. The organic fraction of the plants then degrades relatively rapidly, and the more stable fraction comprising, in the case of grasses, mainly phytoliths, remains. According to Shahack-Gross et al. (2005) an accumulation of a meter of plants would therefore reduce to about 2 cm. The phytolith-rich layers we have examined also contain other minerals such as quartz and clay. Thus, in general, the volume reduction was probably considerably smaller.

Based on the studies of Shahack-Gross et al., (2003, 2005) there are four main criteria for determining whether or not the phytolith-rich layers are from animal enclosures: microlamination, dung spherulites, authigenic phosphate and the types of phytoliths present.

1.1. Ethnoarchaeological background

As the phytolith-rich layers at Tel Dor probably form as a result of plant accumulations degrading or being burnt under domestic or industrial circumstances, one key to understanding this phenomenon is from ethnoarchaeological observations. These are mostly from agro-pastoral societies and unfortunately not from urban contexts that could be more relevant to Tel Dor.

The most comprehensive ethnoarchaeological studies of traditional agro-pastoral societies in the Near East are from western Iran (Kramer, 1982; Watson, 1979) and to some extent from Syria (Kamp, 2000; Roth, 1985) and Ottoman Palestine (Ziadeh-Seely, 1999). Traditional agro-pastoral villages are

basically agglomerates of households (Watson, 1979; Ziadeh-Seely, 1999). Each household consists of an open courtyard and roofed rooms. The rooms are used as the family living room, kitchen, various storage rooms, and as stables for the household's sheep and goats. There are separate stables for cattle, donkeys and horses (Kramer, 1982; Ziadeh-Seely, 1999). Goods stored are grains, straw, and dung cakes. The latter are dried kneaded animal dung formed into flat ovals that are used as fuel (N.F. Miller and P.J. Watson, personal communication; see also Miller, 1984; Reddy, 1998).

Based on the above, accumulations of large quantities of organic materials that could degrade into phytolith-rich layers may occur in abandoned storage rooms (grain and its associated chaff, straw, dung cakes) and in pits, as well as in open areas within and around the site (mostly dung and its ash). As it is unlikely that grain, straw and dung cakes will be left unused, except in cases of abrupt, unplanned, abandonment, the most likely material to form relatively thick phytolith-rich layers of either burnt or un-burnt phytoliths is dung. Note that building with dung today is mostly achieved by mixing dung with mud. This is not expected to form phytolith-rich layers after degradation.

The phytoliths expected to be found in dung of animals maintained by an agro-pastoral society are mainly a mixture of wild and domestic plants. The animals are usually herded away from the site, feeding on wild vegetation, but their diet is supplemented by fodder of both wild and domestic plants. Moreover, it is customary that agro-pastoralists grow plots of plants used as fodder for their animals (e.g., barley in Iran (Watson, 1979); sorghum in India (Reddy, 1997); various legumes and grasses in Palestine (Turkowski, 1969)). In addition, stables are lined with straw, and this is mixed with the dung. The herds often graze on the stubble left in the fields after harvesting the crops. Dung in ethnographic contexts is usually removed from the stables.

Other possible areas of accumulation of plant remains are threshing floors, remains of matting and bedding, roofing of thatch and bark and chaff-tempered mud plaster. Ethnoarchaeological studies emphasize that the straw and chaff (and of course the grains) are collected from the threshing floor (Kramer, 1982; Reddy, 1997; Watson, 1979; Whittaker, 2000). Phytolith layers are therefore not expected to form on threshing floors. This was indeed verified in an ethnoarchaeological study in northern Greece (Tsartsidou et al., in press). Mats and mattresses made of straw would produce thin phytolith layers. Phytolith layers resulting from the decay of woven mats should be composed of phytoliths from reeds or palms; plants known to be used for matting in the Near East. Kramer (1982) also mentions that roofs are lined with reed mats. Upon collapse these may form thin phytolith layers composed of reed phytoliths in a semi-oriented microstructure. Reeds or mats are also occasionally used *inside* mud-brick walls, to bind sections of the wall and/or improve elasticity (Aurenche, 1981). In Uzbekistan straw is placed beneath the roof presumably as insulation (E.B., personal observation). Bark can also be used for roofing (S.W., personal observation, Hunan Province, China). This too would produce a distinctive assemblage of phytoliths and siliceous aggregates (Albert et al., 1999; Albert and Weiner, 2001; Schiegl et al., 1996). Table 1 is a summary of the above data.

Table 1

The phytolith types, presence of spherulites and the microstructure expected to be present in agro-pastoral settlement features, based on ethnographic documentation

Features	Expected phytolith types	Spherulites	Microstructure
Storage rooms			
Straw/hay fodder	D/w, mostly leaf/stem phytoliths	(–)	(?)
Dung cakes	D/W, leaf, stem and inflorescence	(+)	(?)
Grains with chaff	D/w, mostly inflorescence	(–)	(?)
Storage pits (grains)	D/w, mostly inflorescence	(–)	(?)
Open areas (preparation area for dung cakes, livestock paths, etc.)	D/W, leaf, stem and inflorescence	(+)	(?)
Trash heaps (dung and burned dung)	D/W, leaf, stem and inflorescence	(+)	Unoriented ^a
Livestock penning (dung)	D/W, leaf, stem and inflorescence	(+)	Microlaminated ^b
Threshing floors	D/w, leaf, stem and inflorescence	(–?)	(?)
Dung-made installations (chicken coops, hives)	D/W, leaf, stem and inflorescence	(+)	(?)
Matting	W, reed stems, palm leaves	(–)	Thin single layers
Roofing	W/D, wood, grass leaf/stem/inflorescence	(–)	(?)
Bedding	W/D, leaf/stem/inflorescence?	(–)	(?)
Dung plastered floors or walls	D/W, leaf, stem and inflorescence	(+)	Thin separated layers ^c

The features listed are those in which large quantities of organic matter may be present that may degrade into phytolith-rich layers. D/d, phytoliths from domestic cereals; W/w, phytoliths from wild grasses and other wild plants; a capital letter indicates that large amounts are expected and a small letter indicates that small amounts are expected; (+), expected to be present, (–), not expected to be present; (?), empirically unknown.

^a Based on Shahack-Gross et al. (2004) studying a pastoral Maasai trash pit.

^b Based on Shahack-Gross et al. (2003) studying pastoral Maasai livestock enclosures and on Macphail et al. (2004).

^c Based on Shahack-Gross, unpublished data from wall plaster from India and South Africa.

1.2. Tel Dor

Dor was a major port town on the eastern Mediterranean coast (Fig. 1). Its earliest occupation dates to the Middle Bronze Age IIA (ca. 2000–1750 BCE) and its *tell* was continuously and intensely settled until the Roman period (c. 250 CE). Until the building of an artificial port with Roman technology in nearby Caesarea, the natural bays south and north of the *tell* were among the few natural anchorage points along the central part of the eastern Mediterranean seaboard, which ensured the existence of a thriving urban center. This role of a commercial entrepôt is most conspicuous in the early Iron Age—one of the periods investigated in this paper. In contrast to the humble insular material culture typical of this ‘Dark Age’ in the Levant (and elsewhere around the Mediterranean), Dor exhibits certain luxuries, some foreign contacts (with Philistia, Cyprus and Egypt, and to a certain extent with Greece), and it displays dense urban architecture as well as monumental public construction. In fact, architecture has been encountered in every excavation area that reached the early Iron Age strata. For more information on Tel Dor, see Gilboa (2005); Gilboa and Sharon (2003) and Sharon and Gilboa (in press) and a full bibliography at <http://www.hum.huji.ac.il/dor/bibliography.htm>.

The study of phytolith-rich layers thus offers an opportunity to learn more about the use of space both within and outside buildings, and more specifically the manner in which vegetal matter and dung were utilized.

2. Materials and methods

We investigated six phytolith-rich layers from the Late Bronze–Iron Age sequence of Tel Dor in addition to the two

studied previously from the early Iron Age monumental building (area D2, Shahack-Gross et al., 2005). They are located in the following excavation areas (Fig. 1): two in area G, a series of thin layers in area D5 and three in area D2. Table 2 lists the 32 sediment samples analyzed from these areas. They were collected from freshly exposed surfaces using a spatula and placed in plastic vials. We also studied gray powdery sediments that in two cases are juxtaposed to the phytolith-rich layers. For comparison we sampled brown quartz and clay-rich sediments in layers above and/or below the phytolith-rich layers.

2.1. On-site analyses

We used Fourier transform infrared spectroscopy (FTIR) to determine the identities of the major sedimentary minerals. About 0.1 mg of powdered sample was mixed with about 80 mg of KBr, and a pellet was produced using a hand press. FTIR spectra were collected at 4 cm^{–1} resolution using a portable Fourier Transform Infrared (FTIR) Spectrometer (MIDAC Corp., Costa Mesa, CA, USA).

In addition, bulk sediment samples were gently homogenized using a mortar and pestle and a grain mount was prepared using Entellan New (Merck) and examined using a petrographic microscope (Nikon, Labophot2-pol).

2.2. Phytolith analyses

For each sample, a detailed morphometric, morphologic and quantitative study of the phytoliths was performed to identify the types of plants, as well as the plant parts from which the phytoliths were derived. We also address the complicated question of whether or not the plants were from domesticated or wild sources by comparing morphometric traits of the

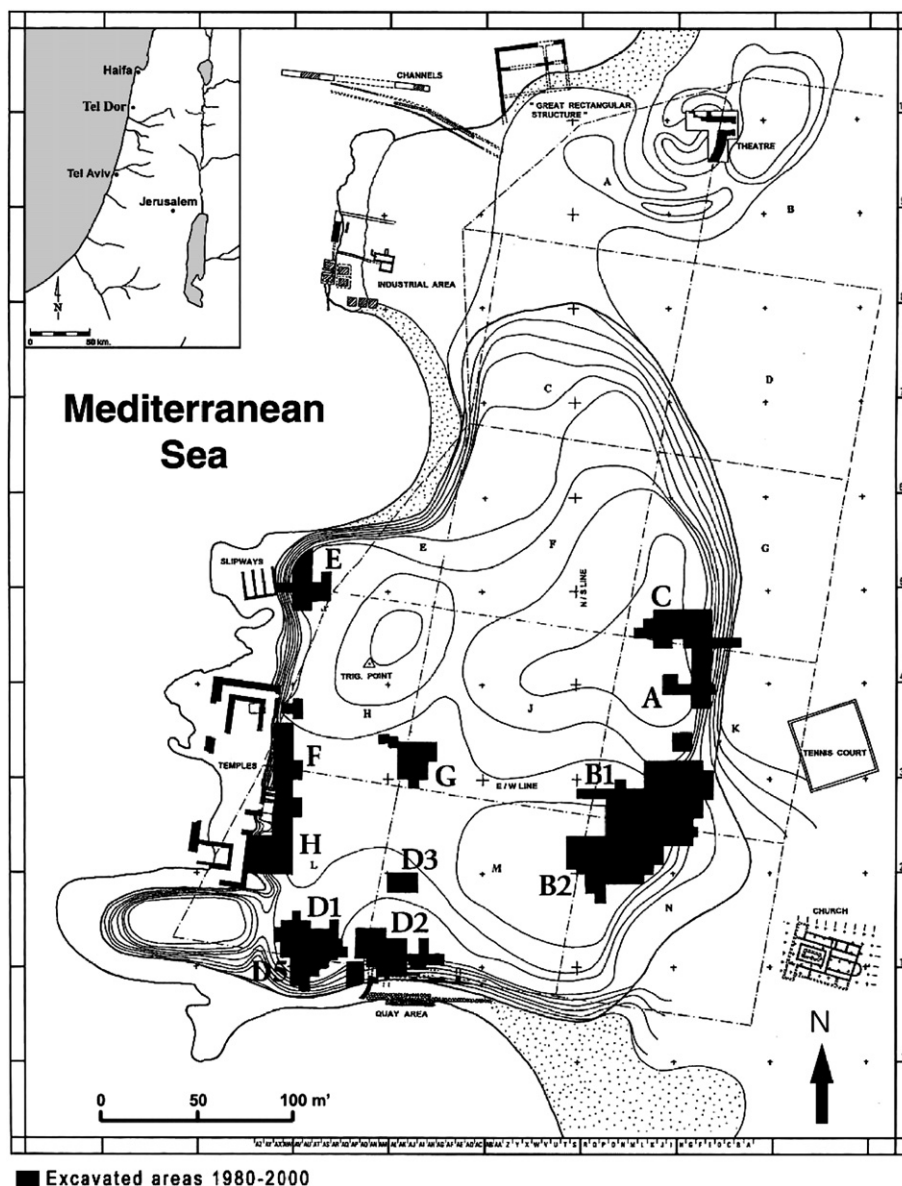


Fig. 1. Map of Tel Dor showing the locations of excavation areas. The current study focuses on six phytolith-rich layers in areas G, D2 and D5. The inset shows the location of Tel Dor on the eastern Mediterranean coast.

phytoliths collected on-site to those of an off-site reference collection.

Quantitative and morphological analyses followed the methods of Albert et al. (1999). Slides were examined using an Olympus BX41 optical microscope and digital images were obtained using an Olympus Camedia C-5060 camera and Olympus DP soft 5.0 software. The number of phytoliths on the slide was counted and related to the original sediment weight. For morphological analysis, a minimum of 200 phytoliths with diagnostic morphologies were counted in order to obtain an error of around $\pm 20\%$ (Albert, 2000).

Morphological identification of phytoliths was based on standard literature (Brown, 1984; Mulholland and Rapp, 1992; Piperno, 2006; Twiss et al., 1969). When possible, the terms describing phytolith morphologies follow anatomical terminology, and otherwise they describe the geometrical

characteristics of the phytoliths. The International Code for Phytolith Nomenclature was also followed where possible (Madella et al., 2005).

Morphometric analysis of phytoliths is an effective tool for differentiating between phytoliths produced by closely related taxa (Ball et al., 1999; Berlin et al., 2003; Pearsall et al., 1995; Zhao et al., 1998). We used "Motic" image analysis software. Ten parameters (Table 3) were measured for the most distinctive inflorescence phytolith morphotype observed, namely dendritic epidermal long cell phytoliths. Thirty phytoliths were analyzed from each sample. We then conducted discriminant analyses (with SPSS for Windows), using calibration data from the same species, following the methodology of Ball et al. (1999) and Berlin et al. (2003).

We measured the refractive index (RI) of the mineral opal in order to differentiate between burnt and unburnt phytoliths,

Table 2
Sediment samples collected in the six localities studied and the results from their phytolith and spherulite concentrations and major mineral components

Sample number	Area	Phytoliths per 1 g of sediment	Spherulites per 1 g of sediment	Refractive index ratio: above/below 1.440	Phytoliths weathering (%)	Major mineral components	Description
32	G loc. 1	6000000	200000	0.67	9.85	O, Q, Cl, Ca	White-gray layer in between 31 and 3
31	G loc. 1	13000000	700000	0.43	9.09	O, Q, Cl, Ca	White layer above sample 32
3	G loc. 1	24000000	800000	0.72	20.8	Q-O, Cl, Ca	White layer below 32
75	G loc. 2	33000000	—	0.25	12	O, Q, Ca, D?	White sediment, lower layer
76	G loc. 2	21000000	—	0.06	14.3	O, Q, Ca, D?	White sediment, lower layer
77	G loc. 2	46000000	—	0.00	11.2	O, Q, Ca, D?	White sediment, lower layer
78	G loc. 2	20000000	—	0.03	8.4	O, Q, Ca, D?	White sediment, wall between stones
79	G loc. 2	100000	—	0.06	21.4	Q, Cl, Ca	Brown sediment, wall between stones
10	G loc. 2	300000	—	0.00	17	O, Q, Ca	White sediment, upper layer
11	G loc. 2	15000000	—	0.00	10.3	O, Q, Ca	White sediment, lower layer
11	D5	7000000	35000	0.03	13.4	Q, Cl, O, Ca	Whitish layer western wall
7	D5	3000000	80000	5	12	Ca, Cl, Q, Ar	Gray sediment western wall
1	D5	9000000	—	0.11	15.5	Cl, Q, O, Ca	Whitish layer western wall
3	D5	300000	—	0.07	5.6	Cl, Q, Ca	Brown sediment western wall
15	D5	1000000	7000	0.00	10.2	Q, Cl, Ca, O	Brown sediment eastern wall below sample 17
17	D5	1000000	300000	0.03	8	Q, Cl, Ca	Brown sediment with Spherulites
17	D2 loc. 1	29000000	—	0.07	15.7	O, Ca, Cl/Q?	White layer
40	D2 loc. 1	14000000	100000	0.07	16.4	O, Ca, D, Cl/Q?	White layer 30 cm from sample 17
41	D2 loc. 1	500000	—	0.03	10.8	Cl, Q, Ca, D?	Brown sediment back side 27 cm from sample 17
112	D2 loc. 2	3000000	200000	0.00	14.3	Q, O, Ca, D, Cl	Brown sediment immediately below white layer
35	D2 loc. 2	11000000	80000	0.07	16.1	O, Cl, Ca	White sediment
36	D2 loc. 2	20000000	40000	0.05	13.2	O	White sediment
69	D2 loc. 2	14000000	400000	1.7	19.2	O, Ca, D, Q?	Gray-loose sediment
43	D2 loc. 2	4000000	400000	0.03	11	Q, Ca, Cl	Brown sediment above white layer
5181	D2 loc. 3	1000000	—	0.03	6.4	Cl, O, Ca	Brown sediment immediately below white sediment
5110	D2 loc. 3	17000000	17000	0.00	16.6	O, Q, Cl, Ca	White sediment
5121	D2 loc. 3	17000000	26000	0.00	13.8	O, Cl, Q, Ca	White sediment
5171	D2 loc. 3	23000000	400000	2	11.6	O, Q, Cl, Ca, D	Gray sediment
5172	D2 loc. 3	6000000	300000	4	12.5	Cl, Q, O, Ca, D	Gray sediment
5035	D2 loc. 3	1000000	100000	0.11	16.3	Cl, O, Ca, D?	Brown sediment immediately above white sediment
39	D1 "control"	30000	—			Cl, Q	Mudbrick
135	D2 "control"	18000	—			Cl, Q	Mudbrick

Ar, aragonite; Ca, calcite; Cl, clay; D, dahllite (phosphate mineral); O, opal; Q, quartz. A refractive index ratio above 1 indicates burned phytoliths and below 1 indicates un-burned phytoliths.

following Elbaum et al. (2003). Slides were prepared using a refractive index medium of 1.440 which is the value that distinguishes burnt from unburnt phytoliths. The ratio between the number of phytoliths with RI >1.440 and the number with RI <1.440 was determined.

A small reference collection of seven modern grass species (divided into their different parts, when possible) were collected in the summer of 2005 from the area of Tel Dor for comparative purposes (Table 4). The methods used to prepare this collection follow Albert and Weiner (2001).

2.3. Micromorphological analysis

Micromorphology was used to better understand the depositional context of each of the layers, and possible post-depositional changes. Undisturbed, oriented sediment blocks were taken from the six localities listed in Table 2. Each of these blocks included the phytolith layer under study and the sediments immediately below and above it. The blocks were

carved out of standing sediment profiles (baulks), coated with Plaster of Paris in order to keep them intact, and embedded in polyester resin in the laboratory. The embedded blocks were sawed into 5 × 7.5 cm sub-blocks from which 30 μm thin sections were prepared. The thin sections were viewed using a polarizing light microscope (Nikon, Labophot2-pol) and described following Bullock (1985) and Courty et al. (1989).

2.4. Analysis of dung spherulites

The number of calcitic spherulites present in each sample was quantified (Table 2). The spherulite quantities in the archaeological sediments were compared to four modern dung samples: two from cattle and sheep in northern Israel and two from goats from southern Israel. The dung was ashed in an oven at 550 °C for 4 h. An accurately weighed aliquot of ca. 1 mg was put on a microscope slide and counted under the microscope as described above for phytoliths. The results show that the spherulite concentrations in modern livestock

Table 3
Morphometric parameters used to characterize dendritic epidermal long cell phytoliths from modern *Triticum* and *Hordeum* species and from archaeological samples

Morphometric parameters	<i>T. dicoccum</i>		<i>T. aestivum</i>		<i>H. marinum</i>		<i>H. vulgare</i>		G loc. 2 77		D2 loc. 2 35		D2 loc. 3 5171		D2 loc. 2 112	
	Mean	STD	Mean	STD	Mean	STD	Mean	STD	Mean	STD	Mean	STD	Mean	STD	Mean	STD
Area	455.1	244.5	258.1	122.5	194.9	75.1	112.6	42.2	332.9	197.9	173.8	74.0	264.1	168.1	287.9	106.5
Convex area	715.3	296.5	451.7	196.9	389.9	168.0	229.2	85.0	581.9	315.0	276.5	111.1	431.1	245.5	490.1	192.6
Perimeter	272.7	66.5	190.4	64.1	196.8	69.7	139.4	40.4	205.1	72.8	138.6	38.7	192.1	86.0	196.5	67.4
Convex perimeter	141.0	29.3	107.2	28.1	97.4	32.2	78.4	24.1	119.5	40.0	74.7	19.8	99.3	38.5	114.1	33.4
Length	57.9	12.9	42.1	13.0	38.1	14.8	31.3	10.9	46.9	19.4	28.2	8.7	38.5	17.6	46.1	16.3
Breadth	15.2	4.0	13.2	3.9	12.3	3.0	9.4	1.8	16.8	5.5	12.0	3.3	13.9	3.5	13.5	3.6
Fiber length	52.8	12.6	37.5	12.7	33.5	15.6	27.7	11.0	41.7	20.2	24.1	8.5	34.4	17.1	41.1	15.2
Width	4.0	2.6	2.6	1.2	2.1	0.7	1.4	0.5	3.2	1.4	3.2	1.4	3.1	1.7	2.9	1.4
Equivalent diameter	58.8	12.8	43.1	12.9	37.7	15.9	32.3	11.0	48.3	19.5	29.1	8.4	39.2	17.3	46.9	16.2
Inscribed radius	29.4	6.4	21.6	6.5	18.9	7.9	16.2	5.5	24.2	9.7	14.6	4.2	19.6	8.7	23.4	8.1

Measurements in μm or μm^2 . The morphometric parameters measured are as follows: area (simple area of the feature); convex area (area within a taut-string around the feature); perimeter (length of the feature boundary); convex perimeter (length of a taut-string around the feature); length (longest cord within the feature); breadth (minimum caliper diameter of the feature); fiber length (length of the feature along its medial axis); width (minor dimension of the feature); equivalent diameter (diameter of a circle with the same area as the feature) and inscribed radius (radius of largest circle that can be drawn in the feature).

dung range between 50 and 350 million spherulites in 1 g of ashed dung.

3. Results

Table 2 lists the samples analyzed, their phytolith and spherulite concentrations and major mineral components. The refractive index (RI) ratio shows whether the phytoliths are burnt or not.

3.1. Structure of the phytolith layers

Micromorphological observations show that phytolith-rich layers may have two different microstructures; a microlaminated structure and an un-oriented, massive, structure (Fig. 2a and b). The former often contains articulated phytoliths, mostly comprising long cells that form clearly defined laminae. All layers include quartz silt and sand grains, clay and calcite to varying extents. Some layers may be centimeters thick (Fig. 2c), others as thin as 1 mm, and in some cases only between 20 and 50 μm (Fig. 2d). Gray layers that are rich in phytoliths are mostly massive with microlaminated domains. They contain large amounts of microscopic charcoal. The gray color is derived from the charcoal. They are thus a product of burned vegetal matter (Fig. 2e).

3.2. Amounts and types of phytoliths

The sediments analyzed have phytolith concentrations ranging from 100,000 to 46 million phytoliths per gram. This can be compared with the 18,000 and 30,000 phytoliths per gram in two mud brick samples (Table 2). An analysis of the phytolith morphotypes shows that in general between 40% and almost 70% of all the phytoliths in these samples are derived from grasses (Piperno, 2006; Rosen, 1992, 1993; Rosen and Weiner, 1994; Twiss et al., 1969). The remaining predominant morphotypes include cylindroids and parallelepiped elongates with smooth or rugose margins. These are characteristic of monocotyledonous plants in general, including sedges, palms, grasses etc. (Albert, 2000; Bamford et al., 2006; Rosen, 1992; Twiss et al., 1969). They are also produced in great numbers in the leaves and stems of grasses (Bamford et al., 2006; Rosen, 1992; Twiss et al., 1969). As no phytoliths indicative of other monocotyledonous families were observed in the samples, and as some of the multicellular structures with smooth margins had short cells from grasses attached, we assume that all the phytoliths with these morphologies were also derived from the leaves and stems of grasses. This implies that the proportion of grasses in the samples analyzed is around 85% or more of all the phytoliths. Phytoliths from the inflorescence of grasses constitute between 40 and 52% of all the phytoliths. This is a relatively large proportion and indicates that, at least in the contexts investigated, whole plants (presumably without roots) were brought to the site (or consumed offsite and deposited onsite as dung or dung-products). A key question for understanding the formation of these layers is whether or not the grasses were derived from wild or domesticated plants.

Table 4
Modern plants analyzed according to their plant parts, and the number of phytoliths per gram of dried organic material

Species	Part of the plant	Number phytoliths per 1 g dried material	Ratio individual/multicellular structures
<i>Avena sterilis</i>	Leaves	700000	2.3
	Stem	100000	0.8
	Inflorescences	200000	1.7
<i>Hordeum bulbosum</i>	Leaves	200000	3.6
	Stem	4000	0.3
	Inflorescences	200000	1.4
<i>Hordeum marinum</i>	Leaves	200000	17.1
	Stem	1000	4.2
	Inflorescences	100000	2.1
<i>Lagurus ovatus</i>	Leaves	100000	9.3
	Stem	4000	4
	Inflorescences	40000	1.2
<i>Hordeum vulgare</i>	Inflorescences	40000	2.5
<i>Triticum dicoccum</i>	Inflorescences	752000	1.4
<i>Triticum aestivum</i>	Inflorescences	40000	1.4

The ratios of single-celled (individual) phytoliths to multi-celled phytoliths are also shown.

3.3. Differentiating between domesticated (cereals) and wild grasses based on phytolith morphologies

This is particularly challenging as short cell phytoliths are abundant in all the samples and they are all derived from the Festucoid sub-family, which includes cereals such as barley (*Hordeum*), wheat (*Triticum*) and oats (*Avena*). Most grass phytolith studies to date focus on phytoliths from the inflorescence to identify the genus, and in some cases even the species. Rosen (1993) and Rosen and Weiner (1994) highlight the importance of a detailed morphological study of papillae cells in conjunction with the type of decoration from the long cells to differentiate between *Hordeum* and *Triticum* in the Near East. Piperno and Pearsall (1993) focus on the short cells of maize in the tropical forests. Berlin et al. (2003) and Ball et al. (1999) performed detailed morphometric studies of long cells with echinate or wavy margins to identify different grass species.

Table 4 lists the reference grass species analyzed, the number of phytoliths per gram of dry organic material and the ratio between individual (i.e., single-celled phytoliths) and multicellular (i.e., multiple-celled or interconnected phytoliths) structures. The latter provides some information on the extent of silicification of the different plants. A correspondence analysis of the different phytolith morphological types among the modern species analyzed, shows that phytoliths vary morphologically depending on the plant part: stems, leaves and inflorescences (Fig. 3). Furthermore, the inflorescences of the domesticated species are differentiated to some extent from the wild species. This implies that there are morphological differences that can differentiate between wild and domesticated grass plants. In general, inflorescences of grasses are represented by more than 40% long cells. In some cases such as *Triticum aestivum* this percentage increases to 72%, and in the wild grass *Lagurus ovatus* it is 11%. More than 67% of the total long cells identified in the inflorescences have decorated margins (dendritic, echinate, wavy, verrucate, etc) (Fig. 4a and b). The exception is *Lagurus ovatus*, where

most of the long cells identified have a smooth or rugose margin. The remaining phytolith morphologies were prickles, papillae and short cells (Fig. 4c and d).

In our limited reference collection, only long cells with dendritic margins are characteristic of domesticated grasses, with one exception (*Hordeum marinum* which is a wild grass). Moreover, only *Triticum dicoccum* has interconnected cells or multicellular structures with dendritic morphologies (Fig. 4e and f). All the other phytolith long cell morphologies are present both in wild and domesticated grasses in different proportions. In our reference collection the proportion of long cells with dendritic margins in domesticated cereals is 7–8% of all the morphotypes present. Thus as a first approximation of the proportions of domesticated and wild grasses present in a given phytolith assemblage, we assume that 7–8% long cells with dendritic margins implies that the grasses were derived entirely from domesticated species, and lesser amounts imply a mix of domesticated and wild species. We note that none of our sediment samples contained more than 7–8% long cell dendritic phytoliths.

In order to obtain a more precise identification of the origin of the dendritic morphology of phytoliths present in the archaeological samples, we performed a morphometric test on several archaeological samples following the method of Ball et al. (1999). The results were compared to those obtained from the modern plant reference collection. Fig. 5 shows that brown sample 112 has dendritic morphologies similar to those in *Triticum aestivum*. White sample 77 and gray sample 5171 also bear a strong resemblance to *Triticum aestivum*. White sample 35 is similar to both *Triticum aestivum* and *Triticum dicoccum*. None of the samples analyzed show similarities to *Hordeum*. The presence of *Triticum aestivum* is consistent with identification of macrobotanical remains recovered from various sites in the region that span the Bronze and Iron ages (Berlin et al., 2003; Borowski, 1987).

Another approach used to identify the type of grass present in the samples and to determine if domesticated or wild grasses are present, is the study of silicified multicellular

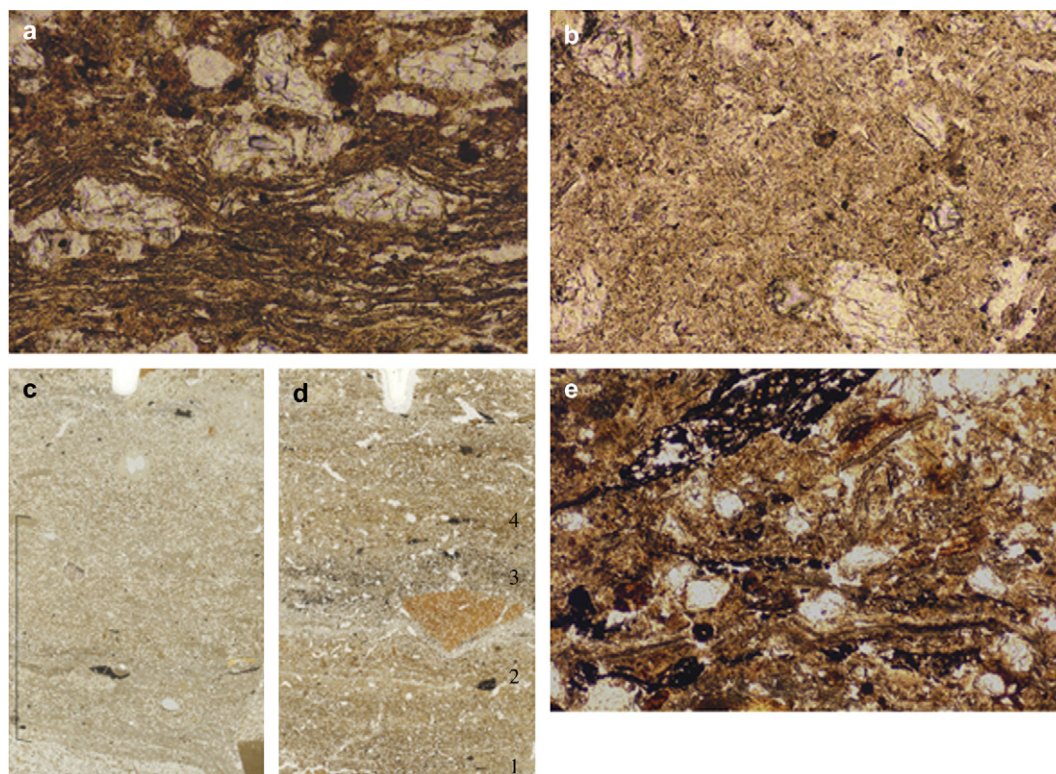


Fig. 2. Mesoscopic and microscopic characteristics of phytolith-rich layers in Tel Dor. (a) Photograph showing microlaminated microstructure from locality D5, plane polarized light (ppl). The large transparent to purplish grains are quartz sand grains. Note that the microlaminae on-lap onto the quartz grains resulting in undulations of the microlaminae. Width of frame is 1.07 mm. (b) Photograph showing un-oriented massive microstructure from locality D2-2, ppl. The large transparent to purplish grains are quartz sand grains. Width of frame is 1.07 mm. (c) Scanned micromorphological thin section from locality G-1 showing a thick accumulation composed almost purely of phytoliths. This uninterrupted accumulation is 3–4 cm thick (marked on the scan). Width of scan is 3.7 cm. (d) Scanned micromorphological thin section from locality D5 showing four thin layers of phytoliths (numbered 1–4) alternating with brown sediment. The layers are between 1 mm thick and up to ca. 5 mm thick. Note that the gray colored layer numbered 3 is burned. Width of scan is 3.5 cm. (e) Microphotograph showing a phytolith-rich gray-colored burned sediment that was identified directly on the white phytolith-rich layer in locality D2-3, ppl. The large transparent to purplish grains are quartz sand grains and the black structures are charred plant remains. The overall microstructure is un-oriented but includes domains of microlaminated phytolith arrays (bottom part of the photograph). Width of frame is 2.14 mm.

structures cells (Rosen, 1992). Our study shows differences in maximum width and shape of waves between *Hordeum* and *Triticum* (Fig. 6a and b). The morphometric analysis shows that most of the long cells that form the multicellular structures in the archaeological samples resemble in maximum width and shape of wave, phytoliths from *Triticum aestivum* (Fig. 6c).

In conclusion, a good approximation of the proportion of domesticated cereals can be obtained from the amounts of long cell dendritic phytoliths, with 7–8% implying that all the phytoliths were derived from cereals. Furthermore, most of the phytoliths from cereals originate from *Triticum*.

3.4. Detailed analyses of the six phytolith-rich layers and associated sediments

Fig. 7 shows the percentages of the most abundant phytolith morphotypes present in each of the samples analysed from the six locations. Note that duplicate or triplicate samples from the phytolith-rich layers were analyzed and the standard deviations are shown. We assume that similar error bars would be obtained

from the other samples. The following are detailed descriptions of the six localities (see Fig. 1 for localities on the tell).

3.4.1. Area G locality 1

3.4.1.1. Archaeological context. This is the thickest phytolith-rich accumulation observed to date at Tel Dor (in places 30 cm or more). It was produced at the beginning of phase G/11 (square AJ32N, locus 18497). The underlying phase, local phase G/12, is the earliest exposed in area G, reached only in two limited probes. It consists of a thick fill with no discernable surfaces and is not associated with any known architecture. The sherds in this fill date it to the Late Bronze Age II (the 14th to 13th century BCE). Phase G/11 also has no architecture in the excavated area, save for one installation—three low stone walls (W18463, W18471, and W18528) framing an area filled with bivalve shells of the genus *Glycimeris*. Other than that, phase G/11 is evident only in a series of superimposed phytolith-rich gray and white layers, generally sloping from northeast to southwest. These were found below the shell-floor installation. Some of the sediments in this phase

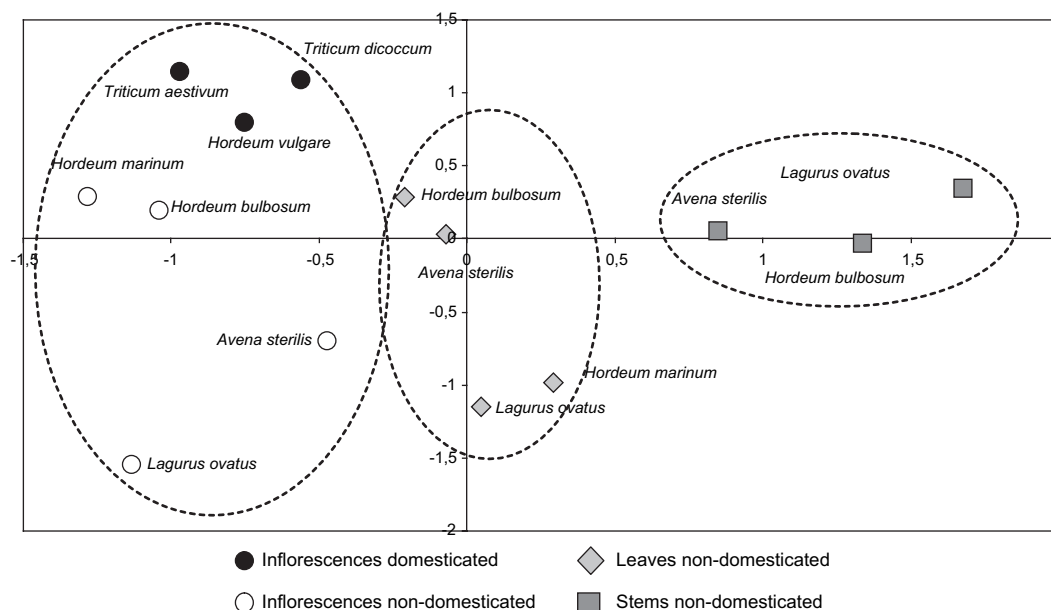


Fig. 3. Correspondence analysis of phytolith morphologies from the modern plant reference collection according to their different parts. Note that the various plant parts tend to cluster and that the inflorescence phytoliths of domestic species can be distinguished from the inflorescence phytoliths of wild species.

are heated sediments in secondary deposition (Berna et al., 2007). The pottery assemblage from phase G/11 mostly dates to a late phase in the Late Bronze Age II (mid-late 13th century BCE). As no real architecture was found in phase 11, we deduce that this was an open space.

3.4.1.2. Micromorphology. A 20 cm long block was extracted at a location where the layer is ca. 12 cm thick. The brown sediment below this layer is composed of quartz sand grains, calcite, clay and artifacts (e.g., ceramics, bones). Its uppermost part contains authigenic phosphate nodules. A densely laminated phytolith-rich layer lies just above the brown layer (Fig. 2c). This layer includes quartz sand grains, calcite, clay, charcoal, wood ash and bones, in addition to many phytoliths. In its lower part calcite seems to have dissolved and in certain places calcitic components such as rock fragments have phosphatic reaction rims. Dung spherulites are not abundant in the section. Certain spherical features ca. 20–50 μm in diameter, are composed of phosphate, which may represent phosphatized dung spherulites. The presence of dissolved calcite and phosphate nodules even below the phytolith-rich layer indicates that degrading organic matter released phosphate and acids that percolated into the sediments below.

3.4.1.3. Phytolith assemblages. The layer was divided into three sub-layers differentiated mainly by color; sample 32 was grayer than the samples immediately above and below (samples 31 and 3). The white-gray sample 32 has less phytoliths and less dung spherulites. Note the abundance of dung spherulites in samples 31 and 3 (Table 2). Morphologically, the three phytolith-rich layers are dominated by grass phytoliths with a high proportion of inflorescence derived phytoliths (Fig. 7). The proportion of dendritic epidermal long cell phytoliths is around 2–4%, implying that less than half the phytoliths were derived

from domesticated cereals. None of these sub-layers contain burned phytoliths. We also noted that the lowest layer (3) contains many weathered phytoliths (Table 2).

3.4.2. Area G locality 2

3.4.2.1. Archaeological context. This phytolith-rich layer (locus F04G-004; Fig. 8a) is located inside a built-up space (room or inner courtyard) that is part of a much larger building complex—a courtyard building of the early Iron Age (Fig. 8b). This structure was first built in local phase G/10 (Ir1ac. early to mid 11th century BCE; for a discussion of the Early Iron Age sequence at Dor and its radiocarbon dating see Gilboa and Sharon (2003), Sharon et al. (2005) and Sharon and Gilboa (in press). It remained in use for a long time and was structurally modified several times (local phases G/9, 8, 7, 6 span the Iron Age I and extend into Iron Age IIA (local terminology: Ir1a to Ir2a), until the 9th century BCE according to the Dor radiocarbon chronology). At the end of phase G/9 the building suffered a major destruction (c. 1000 BCE; e.g., Sharon and Gilboa, in press; Berna et al., 2007) but was quickly rebuilt along the same lines as before.

When sampled, F04G-004 was confined on two sides by walls (W9211 to the north and W9140 to the east). Wall W9140, built of boulders (Fig. 8a in background) overlies another wall built of smaller stones (W9915, barely visible in Fig. 8a). There is also a small but distinct offset between them. These two construction phases were attributed to phases G/9 and G/10 respectively.

The distinct burnt layer of the G/9 destruction (Berna et al., 2007; Sharon and Gilboa, in press) was concentrated in the SE part of the building and gradually decreased towards the north and west. In the sampled room, there was no evidence of fire, but mud-brick collapse of the superstructure was found against

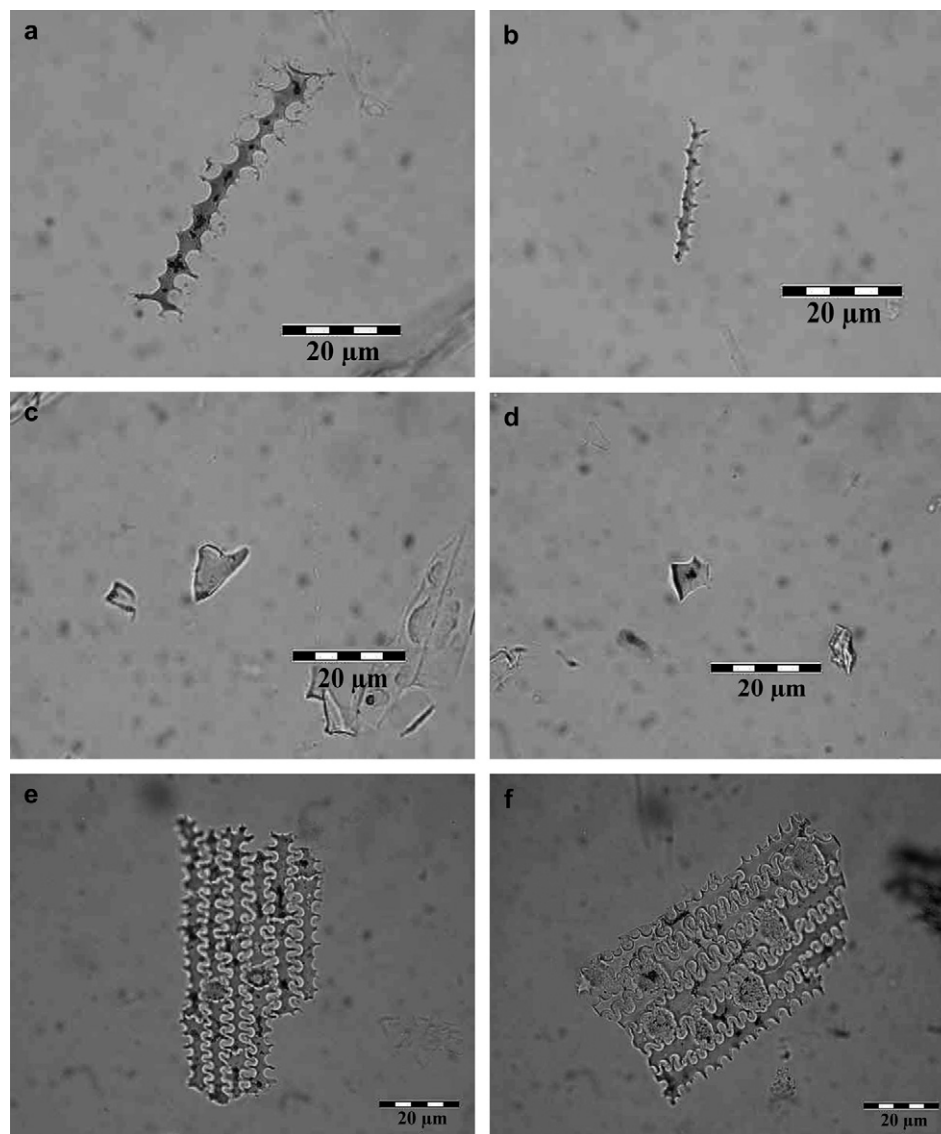


Fig. 4. Photomicrographs of phytoliths from the modern plant reference collection. Pictures taken at 400 \times . (a) Long cell with dendritic margin identified in the inflorescence of *Triticum aestivum*, (b) long cell with echinate margin from the inflorescence of *Triticum dicoccum*, (c) prickle from the leaves of *Avena sterilis*, (d) short cell rondel from the inflorescence of *Hordeum bulbosum*, (e) and (f) multicellular structures with dendritic morphologies from the inflorescence of *Triticum dicoccum*.

the phase G/9 walls. It sealed the phytolith-rich layer and ceramic vessels in primary deposition, though not quite in articulation, in and above the phytoliths. Thus F04G-004 should represent the floor level at the time of the phase 9 destruction. Interestingly, however, the phytolith-rich layer does not abut the bottom of the phase 9 wall, but abuts the underlying wall from phase 10, a few centimeters below its top (Fig. 8a). Thus technically it should be related to phase 10. This in turn implies that an undisturbed phase 9 collapse has no phase 9 living-surface below it. A possible solution to this stratigraphic conundrum may be related to the taphonomy of phytolith-rich layers (see below).

Sifting of the phytolith-rich layer sediment produced dozens of tiny beads—c. 1 mm thick or less—made of gold, copper glass and frit. Below the phytolith-rich layer was a rough flagstone pavement, whose relation to the walls could not be established and below that were more phytolith-

rich layers. The fact that this space was stone-paved is unusual. Elsewhere in Iron Age buildings at Dor, including in monumental constructions, floors were earthen. In the area G building in question, the only other space that was continuously (partially) stone-paved is its central courtyard, which throughout its existence served various industrial activities.

3.4.2.2. Micromorphology. A series of thin (millimeters to centimeters in thickness) white phytolith-rich layers are present, separated by layers of brown clay-rich sediment. The micromorphological section shows two layers both possessing a microlaminated structure. The laminae are dense (ca. 10% voids by area). The two layers contain only small amounts of quartz sand grains (ca. 10% by area), clay and calcite, in addition to the opaline phytoliths. Dung spherulites are notably absent in the section (see also Table 2). Authigenic

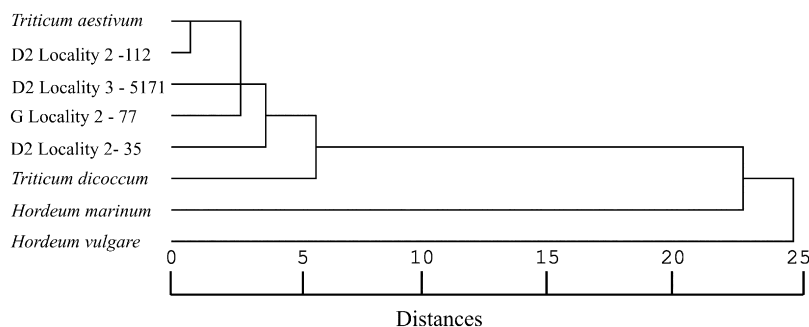


Fig. 5. Comparison of phytolith morphometries between archaeological and modern plant reference collection samples showing nearest neighbor analysis using Pearson's correlation index. The archaeological samples are close to *Triticum aestivum*, with the exception of sample D2 locality 2 35 which is equidistant from both *Triticum aestivum* and *Triticum dicoccum*.

phosphate nodules (composed of dahllite) are present, indicating that organic matter degraded at this location.

3.4.2.3. Phytolith assemblages. The white colored layers contain mainly grass phytoliths with a high proportion of inflorescence derived phytoliths. The phytolith morphotype analyses of the thicker white layers all show that the dendritic epidermal long cell phytoliths constitute between 7 and 8% of all the phytoliths. This is the same proportion present in modern domesticated cereals. Furthermore morphometric analysis shows that these phytoliths are similar to the modern wheat species, *Triticum aestivum*. We therefore conclude that most of these phytoliths were derived from domesticated cereals. Spherulites and other microremains such as starch grains

were not identified in any of these samples (Table 2). Most of the phytoliths have a refractive index lower than 1.440, indicating that these plants were not burnt (Elbaum et al., 2003) (Table 2).

3.4.3. Area D5

3.4.3.1. Archaeological context. This excavated area (phase D5/10) is a large (at least 5×10 m) apparently open space in squares AV/8–10 (Fig. 9). At present it is unclear whether it relates to any architecture. (In the immediate preceding and subsequent phases in this area (respectively D5/11 and D5/9), this space is bounded by walls. The three rubble walls in Fig. 9 belong to phase D5/9 and cut the sediments analyzed here).

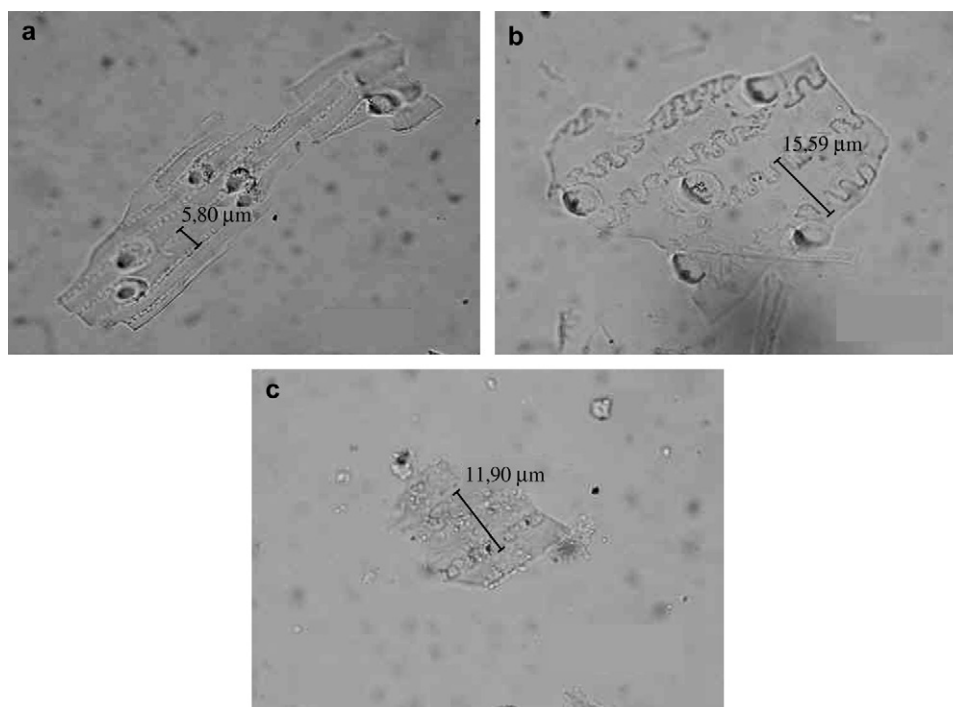


Fig. 6. Photomicrographs of silicified multicellular structures showing the differences in maximum width and shape of waves between *Hordeum* and *Triticum*. (a) Multicellular structures of long cells with wavy margin from the inflorescence of *Hordeum vulgare*. (b) Multicellular structures of long cells with wavy margin from the inflorescence of *Triticum aestivum*. (c) Multicellular structures of long cells with wavy margin from archaeological sample 5171.

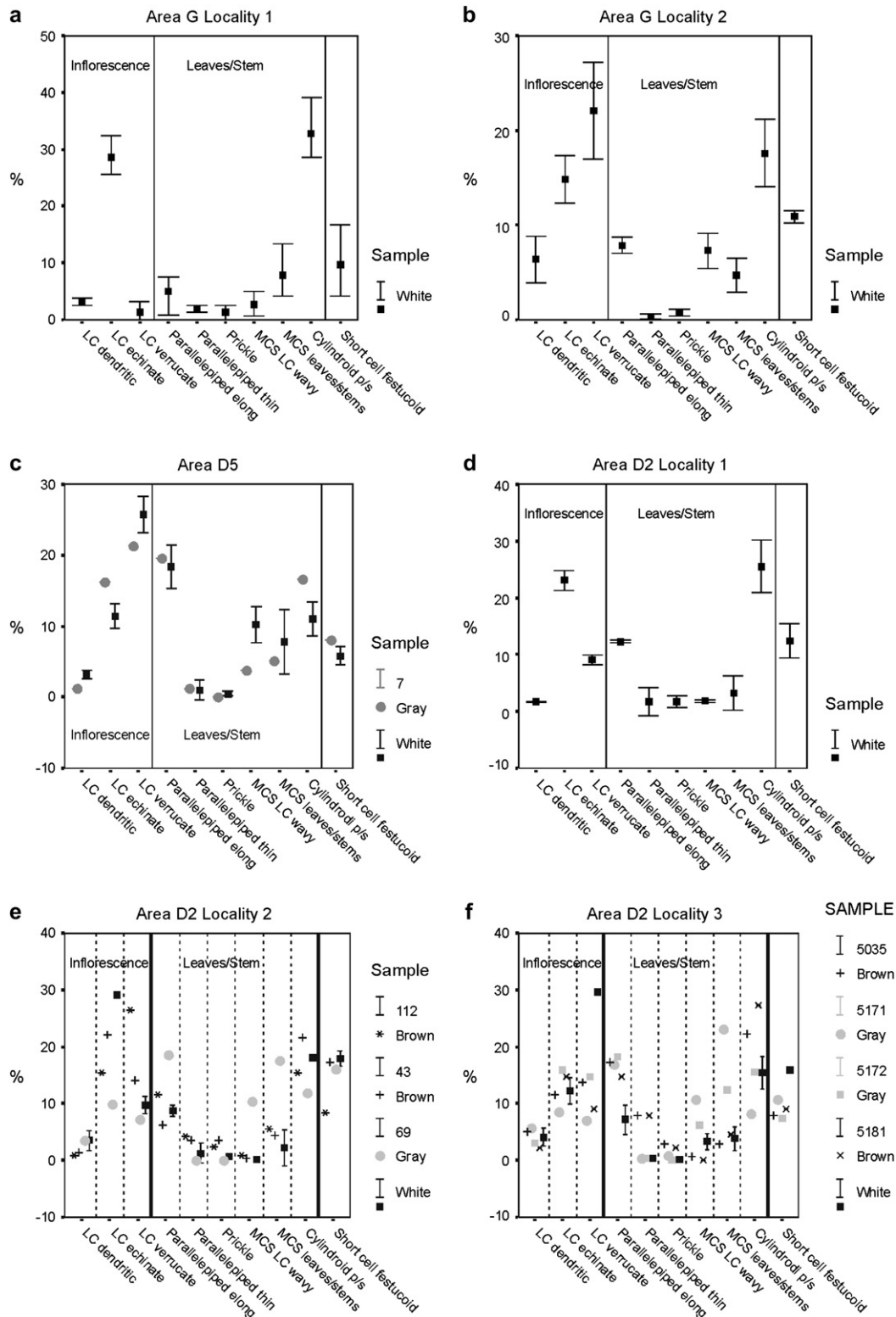


Fig. 7. Plots showing the percentage of the phytolith morphologies identified in the six localities analyzed. This percentage includes only those morphologies that exceed 2% of the total phytolith record. White sediments from a same locality are plotted together showing the average with the standard deviation bar (see Table 2 for description of samples). Each plot is separated according to the provenance of the different phytoliths morphological types in the plant (inflorescence, leaves/stems and non-specific plant part). LC, long cells; MCS, multicellular structures; p/s, psilate/scabrate margin.

Phase D5/10 dates to the Iron Age I/II transitional phase (Ir1|2 in Dor terminology, c. 900/880 BCE, by the Dor radiocarbon sequence). The whole area consists of a series of thick and thin

phytolith-rich layers. At the macroscopic level, the white phytolith layers are interspersed with dark brown mud-brick material. The layers are extremely uneven. The entire series is



Fig. 8. Area G locality 2. (a) The phytolith-rich layer exposed in area G locality 2; (b) section through the phytolith layer showing how it on-laps onto the adjacent wall (arrow).

as thick as 1 m in places. It generally slopes from north to south in a series of distinct ‘steps’ as well as sloping from west to east in a less dramatic fashion. Moreover, the center of the area forms a trough-like depression, as wide as 1 m and 50 cm deep. One part slopes from north to south and another to the east, to form a sunken “T” shaped feature (Fig. 9). Abundant ceramics in all these layers comprised small potsherds only, and bones, obviously in secondary deposition. Immediately below the series of phytolith-rich layers is a heavily burnt destruction layer (phase D5/11) containing many *in situ* pots dating to the Iron Age I.

3.4.3.2. Micromorphology. A 25 cm long block was extracted that included alternating white-brown sediments and uniformly brown sediment above. Thirteen distinct phytolith-rich layers over a total thickness of 20 cm were identified. Their thicknesses vary between 1 and 10 mm. One of these layers appears to be burnt based on the abundance of charcoal and calcitic ash. The thickness of the brown sediment between these layers varies between 5 and 15 mm. All layers are microlaminated, but with different phytolith densities, i.e., some show compacted phytoliths stacked one on top of the other, and others show an accumulation of white fiber-like micro-layers alternating with brown material. The overall porosity

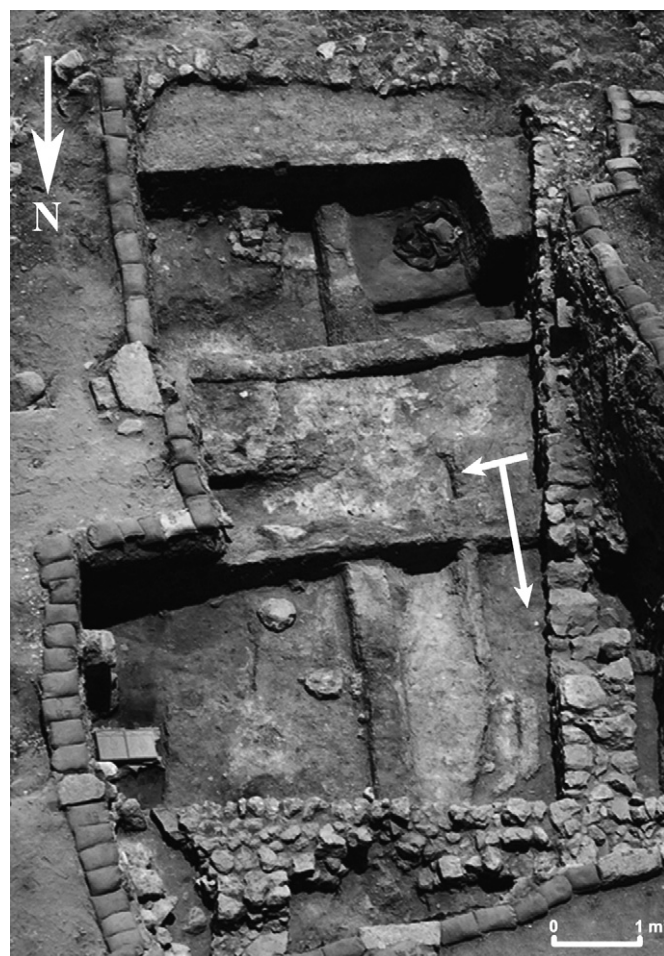


Fig. 9. Aerial photograph of the area D5 phase D5/9 showing the two orthogonal trough-like structures (arrows) with phytolith-rich layers exposed.

of these layers varies between 10 and 30% of void areas. Usually a 10% void area corresponds to high phytolith densities. Other materials identified in some of the phytolith layers, include dung spherulites, microscopic bones, burnt clay, charcoal and ash, in addition to the usual quartz sand grains, clay and calcite (Table 2, Fig. 2d).

3.4.3.3. Phytolith assemblages. Phytoliths were well preserved and more abundant in the white and gray samples as compared to the brown samples. The refractive index ratio is always below 0.1 indicating that the phytoliths were not burnt. The exception is the gray colored lens (sample 7), where the phytoliths have a refractive index ratio of 5 (Table 2) and are therefore burnt. Grasses represent more than 91% of the total phytolith count, and the proportions of phytoliths from the inflorescence parts are relatively high. The exception is sample 17, which has an inflorescence content of 26%. The proportion of dendritic epidermal long cell phytoliths is between 1 and 4%, implying that, at most, about half the phytoliths were derived from domesticated cereals. We also noted the presence of a few short cells of bilobates, either from C4 grasses or in sample 17. The grasses are derived from both

wild and domesticated plants. Dung spherulites are present in the white and gray powdery samples, but are more abundant in brown sample 17.

3.4.4. Area D2

We analyzed three phytolith-rich layers from this area (Fig. 10, localities 1, 2 and 3). All are ascribed to phase D2/6. Phase D2/6 is composed of a series of occupation surfaces, pits and depressions which cut the massive ashlar architecture and crushed *kurkar* floors of phase 7 (Iron Age IIA, 9th century BCE). The general character of phase D2/6 indicates an open area, dotted by refuse pits. It is quite long-lived, spanning the Iron Age IIB (8th century BCE) and Iron Age IIC (7th century). During this time pits were filled in, often with alternate layers of different materials, and new pits were dug, sometimes cutting earlier ones. The different ages of the sub-phases are sometimes discernable stratigraphically and sometimes by the relative typology of the ceramic assemblages within them.

3.4.5. D2 locality 1

3.4.5.1. Archaeological context. This phytolith-rich layer was found over an area of some $4 \times 4 \text{ m}^2$ (square AO12, locus L04D2-023) (Fig. 10, L 1), and in one place it was draped over a group of fairly large fallen stones. There is no evidence that this layer was part of a pit or dumping area. This phytolith-rich layer forms one of a series of more-or-less horizontal surfaces which underlie phase D2/5 (Persian period) walls in AO12 and seal the crushed *kurkar* surfaces that reach the ashlar walls of phase D2/7. Thus, by default, the phytolith-rich layer should be considered a phase 6 feature, though there is no stratigraphic link between it and the phase 6 pits in AM14–AO14 (discussed below). The ceramic horizon indicated by their contents is unclear: somewhere in the 9th to 8th century BCE range. No architecture is associated with phase D2/6 in this unit. The best assessment is that this was

an open area, littered with stones and other debris from the collapse of previous structures.

3.4.5.2. Micromorphology. A 15 cm long block was examined that includes brown sediment below the white layer. The latter is overlain by gray sediment. The white phytolith-rich layer, ca. 10 cm thick, has a massive and compact microstructure (Fig. 2b). It has vertical voids (channels) through which water drained downwards. Calcite hypocastings are present around the voids, and movement of quartz grains along the vertical drainage channels is also evident. The drainage channels caused fragmentation of the phytolith-rich layer. Intact domains of the phytolith-rich layer found between the drainage channels have ca. 5% voids by area and ca. 10% quartz grains by area. The layer also contains calcite and clay, small amounts of charcoal and fragments of bones, shells, burned *kurkar* and pottery. There are several small domains that possess a microlaminated structure. Dung spherulites, as well as phosphatized spherulites and phosphate nodules are present in the section. These data indicate that the layer is derived from dung and it resembles the layer described below for D2 locality 2, square AO14.

3.4.5.3. Phytolith assemblages. The phytolith assemblages of the two white samples are very similar, but the brown sample from associated sediment is significantly different both in number (Table 2) and morphology (Fig. 7). Only one of the white samples however contained spherulites. The refractive index ratio is below 0.1 in all three samples indicating that the phytoliths were not burnt. The assemblage of phytoliths is similar to that found in locality 2, square AO14 (see below) although with a lesser proportion of dendritic long cell phytoliths, which is around 2%, implying that most of the phytoliths were derived from wild grasses.

3.4.6. D2 locality 2

3.4.6.1. Archaeological context. This phytolith-rich layer covers a relatively large area (square AO14, locus F04D2-063) (Fig. 10, L 2), and follows the underlying surface topography. The latter was formed by two large pits dug prior to the deposition of the phytolith-rich layer. Pit L05D2-544 is the earlier of the two. After it was filled in, another pit (L05D2-517) was dug, partly cutting into L05D2-544. Both pits cut the large ashlar wall W04D2-065 of phase D2/7 and its associated crushed-*kurkar* floors. The phytolith-rich layer studied in detail covered pit L05D2-544 more-or-less horizontally, but then sloped sharply (at one spot almost vertically) into pit L05D2-517 where it continued at a lower elevation. There is no direct stratigraphic link between the pit-complex in AN-AO14 and that of AM14, but the pottery horizon of the entire AO14 complex (including the potsherds found in the phytolith layer itself), is definitely early in phase D2/6 (Iron Age IIB (8th century BCE) rather than Iron Age IIC (7th century). The nature of the fill-layers is also different. The AO14 pits contain far less pottery than the AM14 7th century pit (below). It represents a ‘mundane’ household

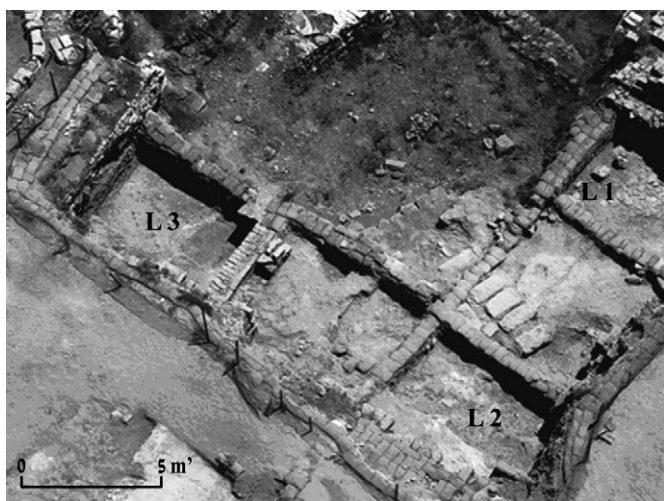


Fig. 10. Aerial photograph of area D2 showing the locations of the three phytolith-rich layers studied. (a) Locality 1, square AO12; (b) locality 2, square AO14; (c) locality 3, square AM14. The excavation squares are $5 \times 5 \text{ m}$.

assemblage, mostly not in primary deposition, and little or no metallurgical wastes.

3.4.6.2. Micromorphology. Two blocks were collected. One includes the white phytolith-rich layer and the associated brown sediments, and the other a phytolith-rich powdery gray sediment. This block overlies the white phytolith-rich layer in certain places. The white layer possesses a massive, un-oriented, microstructure. It is very compact (5% voids by area) and includes quartz sand grains (10% by area), small amounts of clay, calcite, microscopic bones (some are burnt), and probable burnt mud-brick fragments. It also includes authigenic phosphate nodules that extend to the brown layer below. The gray powdery layer was sampled in the deepest part of the feature. The gray layer possesses a microlaminated structure that is usually not continuous over many centimeters, probably because this layer is very porous (30% voids by area) possibly promoting the collapse of the original microstructure. The gray layer is composed almost entirely of phytoliths. It also includes quartz sand grains (5% by area), clay, calcite, and many charred vegetal remains. Certain rounded silicate grains are amorphous and have a bubbly appearance, and one quartz grain was identified as having an amorphous rim. These properties indicate that the organic matter burnt at a rather high temperature. Other burnt materials found in this layer are calcite nodules, mud-brick and/or ceramic fragments. The layer includes authigenic phosphate nodules.

3.4.6.3. Phytolith assemblages. Two samples from the white phytolith-rich layer were analyzed. The gray sample was located on top of the white layer. One brown sediment sample was analyzed from immediately above the same white layer (Table 2). Grasses dominate the phytolith assemblage in all the samples. The proportion of dendritic epidermal long cell phytoliths in both the white and the gray samples is between 3 and 4%, implying that about half the phytoliths were derived from domesticated cereals (Fig. 7). The refractive index ratio of the phytoliths is below 0.1 in all the white and brown sediments and above 1.7 in the gray samples. The phytoliths in the latter are therefore burnt. The white layer contains a relatively high proportion of phytoliths from the inflorescence, and a small number of spherulites (Table 2). The phytolith assemblage from the gray sediment differs from that of the white sediment (Fig. 7), aside from being burnt, by having proportionately more leaf phytoliths than the white layer and many spherulites (Table 2). The brown sediment above the white layer contains relatively high concentrations of phytoliths compared to other clay-rich brown layers, and large amounts of spherulites.

3.4.7. D2 locality 3

3.4.7.1. Archaeological context. This area was part of a very large (about 100 m²) pit that was dug into a mud brick layer (square AM14, loci L05D2-808 and L05D2-801) (Fig. 10, L 3). The abundant pottery dates it to the Iron Age IIC; mostly the late 8th/first half of 7th century BCE. This corresponds

to the Assyrian occupation period of the Levant. Indeed, the pottery is the most remarkable macroscopic aspect of this pit. Some of the layers seem to be composed almost exclusively of large potsherds, many of which could be mended to form complete or near complete vessels. Almost all of these are of two specific types; short-necked straight-shouldered transport jars typical of the 7th century BCE. These are abundant in Phoenician entrepôts across the Mediterranean; and small, crudely formed jugs of an uncommon type, both at Dor and elsewhere. The pit also contains abundant debris from metallurgical industries and two distinct phytolith-rich layers. Here we examined the lower phytolith-rich layer (locus L05D2-808) which is overlain, in many places, by a gray powdery phytolith-rich sediment (locus L05D2-801), which is clearly thicker in the depressed areas. The powdery gray layer forms the base of a burnt assemblage of sedimentary minerals that is over 30 cm thick. In addition to the pottery, many bones were closely associated with the phytolith layers.

3.4.7.2. Micromorphology. The white phytolith-rich layer has a dense microlaminated structure. The layer is ca. 3 cm thick with about 10% of voids. The layer contains mainly phytoliths, quartz sand grains (ca. 5%), calcite and clay, and in addition, pottery sherds, shell fragments, kurkar fragments, burnt bones, plaster, and a rounded grain of basalt. Small spherical phosphatized features may be phosphatized dung spherulites. Phosphate nodules are present. They are abundant at the upper centimeter of the layer.

The gray layer immediately above the phytolith layer is ca. 8 cm thick and generally has a massive structure except for areas where charred fibers are horizontally oriented (Fig. 2e). It is relatively porous (ca. 20% voids by area). This layer has more calcite than the layer below and also includes clay and quartz sand grains (the latter comprise some 10% by area). Artifacts in this layer are fragments of pottery, burnt bones (some of them calcined), possible glass, charcoal, burned kurkar fragments with unburnt cores, mud brick fragments, plaster fragments, chalk and one rounded clay curl. Towards the top of this layer is a sub-layer ca. 1 cm thick of articulated microlaminated phytoliths derived from burned grass.

3.4.7.3. Phytolith assemblages. Two samples from the white phytolith-rich layer were analyzed. The two gray samples were located on top of the white layer and were separated by a few centimeters. One brown sediment sample was analyzed from immediately below the white layer and another from immediately above the same white layer (Table 2). Phytoliths are abundant in the white and gray colored samples. The phytolith assemblages are similar in the two white phytolith-rich samples, but are different in the gray and brown samples. The two gray samples have different assemblages, even though they are separated by only a few centimeters (Fig. 7). The refractive index ratio indicates that phytoliths were not burnt in the white and brown samples but were burnt in the gray samples. Spherulites are present in small amounts in the white phytolith-rich samples, and are abundant in the gray samples. They were also present in the brown samples

(Table 2). Grasses dominate the assemblages (above 89% of the total counting). The proportions of inflorescences is highest in the white samples (54%), slightly lower in the gray samples (38–43%) and lowest in the brown samples (26–34%). The long cells dendritic phytoliths of both the white and gray layers constitute about 3–5% of the total assemblage. The phytoliths in these layers were therefore derived from a mix of both wild and domesticated grasses. The gray samples contain a small but significantly larger amount of leaf phytoliths as compared to the white samples.

4. Discussion

The phytoliths from the phytolith-rich layers are almost all derived from grasses, with a relatively high proportion from the plant inflorescence. The gray layers all contain burnt phytoliths and a higher percentage of phytoliths from grass leaves, whereas the white layers are not burnt and inflorescence phytoliths are, in general, more abundant. At this level the analyses of the 6 phytolith-rich layers present a rather uniform and consistent picture. There are however significant differences. These are summarized in Table 5.

Three out of the six phytolith-rich layers (area G loc. 1, area D5 and area D2 loc. 3) have properties consistent with having originally been formed from dung in animal enclosures. These are a microlaminated structure indicative of trampling by animals (Shahack-Gross et al., *in press*), phosphate nodules indicative of the breakdown of organic materials, dung spherulites produced in the digestive systems of certain herbivores, especially abundant in area G loc. 1, and phytoliths derived from a mix of both domesticated and wild grasses. We know from ethnography that a mix of wild and domestic grasses is widely used as animal fodder.

The two phytolith-rich layers in area D2 (localities 1 and 2) differ from the others by having a massive rather than a laminated microstructure. Dung spherulites are either absent or present in low numbers, especially when compared to the gray sediments immediately above (area D2 locality 2). The reason for the low number of dung spherulites could be explained by diagenetic processes (see below). The massive structure is more consistent with animal dung having been re-deposited in these locations. It is possible that the massive structure may indicate localities of dung cake preparation or other activities using dung as a construction material as wetting and churning of dung as a first step in molding dung into specific (macro) structures is a process that probably results in random orientations of the plant fibers in the dung.

The phytolith-rich layer from area G locality 2 presents properties that cannot be interpreted unequivocally. The microlaminated structure implies that this layer resulted from trampling. It is within or on the side of a small paved room floor, includes only cereal phytoliths and dung spherulites are absent. Authigenic phosphate nodules are present, indicating that organic matter degraded at this location. If this was a storage area for cultivated crops, then the presence of a microlaminated texture remains unaccounted for. There is no parsimonious explanation for the formation of this layer.

Concentrations of dung spherulites in modern samples are very high (they range between 50 and 300 million per gram of ashed dung) in relation to the concentrations found in the archaeological sediments (Table 2). This may be due to diagenesis. Spherulites are susceptible to dissolution, especially as the pH becomes acidic when large amounts of organic matter degrades (Canti, 1999). This could even differentially affect the spherulites as compared to the calcite which is present in many of these samples, usually in small amounts. This is deduced from Shahack-Gross et al.'s (2003) observation that the spherulites are initially formed from monohydrocalcite and not calcite. The former is much more soluble than calcite. We also noted phosphatic spheres in the range of sizes that is similar to that of dung spherulites, thus indicating that phosphatization of dung spherulites may occur due to diagenesis in an environment rich in phosphate. Dung spherulites are totally absent from the area G locality 2 phytolith-rich sample. Dung spherulites are produced by many animal species (Canti, 1997) but are known to be present in large amounts in ruminants, i.e., cattle, sheep and goats. A zooarchaeological study in Tel Dor showed that the majority of faunal remains were from sheep and/or goats (Gerstel-Raban, *in press*). Thus spherulites should be present in dung accumulations.

Gray powdery phytolith-rich layers have phytolith assemblages that are burnt and they contain dung spherulites. Micromorphological analysis shows that the gray color is due to the presence of charcoal. Their presence indicates that dung may have been burnt as fuel and that its ash was dumped at the localities studied here. The presence of small domains of microlaminated structure is puzzling, as we do not expect it to preserve if the dung ash is re-deposited. The other possibility is that the dung was burnt *in situ* and that its structure collapsed into the many voids evident in these gray sediments (see micromorphological descriptions above). However the phytolith assemblages in the gray sediments differ from those in the white layers at the same localities. This is consistent with the gray sediment not being burnt *in situ*. Moreover, the presence of microlaminated domains together with high porosity in the gray sediments indicates that these sediments were not trampled after deposition as this would probably destroy the lamination and reduce the porosity. It seems that the white and gray layers reflect different uses of the same area, albeit, at least in some areas, both involving animal dung. Note however, that we observed one thin phytolith-rich gray layer (Fig. 2d layer number 3) whose structure was microlaminated throughout, probably indicating that it was burnt *in situ*.

The absence of phytoliths from reeds or from palm trees implies that none of the phytolith-rich layers we have sampled to date are derived from matting. The mix of wild and domestic grasses is also inconsistent with the phytoliths being derived from thatched roofing, which is usually built from the stems of domesticated cereals.

4.1. Taphonomic implications

In the area G locality 2, all the phytolith-rich and associated layers slope sharply upwards towards the walls (Fig. 8). This

Table 5
Summary of main results obtained for each of the six studied localities

Locality	Archaeological context	Macroscopic features	Microlaminated?	Burnt?	Spherulites	Domestic vs. wild	Inferred activity
Area G: 1	Bronze Age, open area	5–30 cm thick series of white sediment	Yes	No	Yes	D + W	Long term livestock penning
Area G: 2	Iron Age, small room related to a large residential building	5 cm of brown sediment incorporating two separated white layers ca. 0.5 cm thick each	Yes	No	No	D	No parsimonious explanation
Area D5	Iron Age, probably courtyard related to a building	A series of thin white or gray layers alternating within brown sediment	Yes	White, no; gray, yes	Yes	D + W	Short episodes of livestock penning, occasional burning,
Area D2: 1	Iron Age, open area	White layer 2–3 cm thick	No	No	Yes in 1 white layer	D + W	Redeposited dung; trash or dung-cake preparation area?
Area D2: 2	Iron Age, open area, series of pits	Gray powdery layer, variable thickness	Yes (in domains)	Yes	Yes	D + W	Burned dung
		White layer 2–4 cm thick	No	No	Yes, lesser amount	D + W	Redeposited dung; trash or dung-cake preparation area?
Area D2: 3	Assyrian period, open area, a large trash pit	Gray powdery layer, variable thickness	Yes (in domains)	Yes	Yes	D + W	Burned dung
		White layer 2–3 cm	Yes	No	Yes, lesser amount	D + W	Change of use from trash pit to livestock enclosure and back to trash dumping area

D, domestic grasses (possibly wheat); W, wild grasses.

could be due to subsidence of the floors. In fact if other phytolith-rich layers are present deeper in the section, this would explain why the floors found directly under the phase G/9 mud-brick collapse seem to reach a phase G/10 wall. In area D5, the phytolith-rich layers as well as the associated layers have arc-like subsidence features which correlate with existing robber-trenches. Thus the compression of the organic-rich sediments presumably followed the underlying topography defined by the robber trenches. In area D2 locality 2 the phytolith-rich layer also followed the pre-existing pit topography and at one location was almost vertical. In locality 1 they were draped over the surface of a series of large rocks, which must have been under the organic-rich sediments. All these phenomena can be explained by the taphonomic degradation of a thick organic-rich layer that leaves a relatively thin residue on the substrate. Such large volume reductions of organic-rich sediments can result in artefacts changing their stratigraphic positions relative to the architecture. They can also cause concentrations of artefacts that were originally separated.

4.2. Cultural implications

Phytolith-rich layers were found at Dor in open spaces between houses, courtyards within houses, roofed spaces within

houses, refuse pits, and even in monumental public structures. Their presence on the *tell* indicates an intimate association between humans, animals, plants and bio-waste products, such as chaff, straw, unconsumed animal fodder, and animal dung during the Late Bronze Age and Iron Age. Thus open lots and/or unoccupied structures within the town were used as animal enclosures or for the disposal of organic-rich waste products. This may well have implications for estimating population size from the site area, herd size for individual enclosures or even the very assumption of a “stratum”, namely that all structures within the stratum were in use at the same time.

A broader question arises from the association between humans, animals and plants in an urban context. It is noteworthy that all of the ethnographic parallels referred to in the introduction are from agro-pastoralist villages. In towns in the present-day Near East, even traditional ones, animal and vegetal materials are mainly introduced as more-or-less processed consumer goods. Thus the patterns of co-habitation of humans with animals, their food and their dung are significantly different than that observable in villages. Dor however was an urban center throughout the period under study. Indeed, in one of the sub-periods, the Iron Age I, a ‘dark age’ around the entire Mediterranean, Dor is one of the few flourishing urban centers, boasting massive fortifications and monumental public structures.

Chronologically the phytolith-rich layers range from the Late Bronze Age (13th/12th century BCE) to the end of the Iron Age (7th century BCE). Although we have not systematically surveyed all exposures on the *tell*, phytolith-rich layers are almost totally absent in the later Persian, Hellenistic and Roman strata. This in turn might indicate a major change in the urban environment following the Iron Age, and perhaps the very definition of a city (*urbis*) itself. Some time between the end of the Iron Age and the onset of the Hellenistic period, a dichotomy was created between ‘village’, where agricultural goods are produced and humans cohabitate with animals, plants, and their waste products, and ‘city’ as the realm of a consumer society. There are clues that this indeed may be the case. For instance, it has often been noted that biblical Hebrew has no word to denote ‘village’. Any habitation larger than an isolated farm is a ‘town’. Mishnaic Hebrew (i.e., during the Roman period) already possesses a separate word for ‘village’.

Archaeologists are used to thinking in terms of a single ‘urban revolution’, which happened in the case of the Levant at the beginning of the third millennium BCE. It consisted of the nucleation of settlements in which supra-subsistence activities (trade, storage and re-distribution, craftsmanship, ritual, government, etc.) are centered. Our evidence suggests that in Dor at least, households remained a locus of primary food production, with the attendant biogenic wastes. This is also indicated by a recent analysis of the early Iron Age faunal assemblage of area D2 (Gerstel-Raban, in press), in which parameters like the distribution of (mostly domesticated) animals, age and gender distribution, body-part representation, butchering, filleting and skinning marks, and more, indicate that meat was not only consumed at Dor, but also produced there. If the observations at Dor are representative for these periods, then the second ‘urban revolution’ which pushed primary food production and its wastes out of the town altogether or at least proscribed it to specific spaces (markets, public stables, etc.), might have coincided with the Hellenization of the Levant. (See for example Morris (1991, p. 40) and Whitley (2001, p. 174) for a similar and largely contemporaneous process in Greece, i.e., ‘real’ urban space taking shape not before the late 6th century BCE.) It is clear that the elucidation of the physical and social matrix which we customarily designate as an early Levantine town or city will have to reach beyond architectural analyses (Herzog, 1997).

5. Conclusions

This study shows that layers composed mainly of phytoliths can form. At Tel Dor they are for the most part the product of the break down of animal dung. This dung accumulated either in animal enclosures, or was redeposited under circumstances that are not well understood. The transformation of the dung accumulation into a relatively thin layer of phytoliths is accompanied by significant reduction in volume and hence can cause subsidence of the overlying strata. This may complicate stratigraphic relations in the field. Finally the identification of many such dung accumulations and hence animal

enclosures on the *tell*, raises questions about the style of life of the *tell* inhabitants during these periods and the nature of urbanism at this time.

Acknowledgements

We thank the area supervisors Elizabeth Bloch-Smith, Willem Boshoff, Yiftah Shalev and Avshalom Karasik. We also thank the Berman Center for Biblical Archaeology, Mr George Schwartzmann, Sarasota, Florida, and the Kimmel Center for Archaeological Science for their financial support. R.S.G. would like to thank Liora Kolska-Horowitz for providing a sample of dung plastered wall from South Africa, reported in this study. S.W. is the incumbent of the Dr Trude Burchardt Professorial Chair of Structural Biology. The Fundación Atapuerca financed the research performed by D. Cabanes.

References

- Albert, R.M., Lavi, O., Estroff, L., Weiner, S., Tsatskin, A., Ronen, A., Lev-Yadun, S., 1999. Mode of occupation of Tabun Cave, Mt Carmel, Israel during the Mousterian period: a study of the sediments and phytoliths. *Journal of Archaeological Science* 26, 1249–1260.
- Albert, R.M., 2000. Study of Ash Layers through Phytolith Analyses from the Middle Paleolithic Levels of Kebara and Tabun Cave (Israel). University of Barcelona, p. 250.
- Albert, R.M., Weiner, S., 2001. Study of phytoliths in prehistoric ash layers using a quantitative approach. In: Meunier, J.D., Colin, F. (Eds.), *Phytoliths: Applications in Earth Sciences and Human History*. A.A. Balkema Publishers, Lisse, Netherlands; Exton, PA, pp. 251–266.
- Aurenche, O., 1981. *La Maison. Orientale: l’Architecture du Proche Orient Ancien des Origines au Milieu du Quatrième Millénaire*. P. Geuthner, Paris.
- Ball, T.B., Gardner, J.S., Anderson, N., 1999. Identifying inflorescence phytoliths from selected species of wheat (*Triticum monococcum*, *T. dicoccum*, *T. dicoccoides*, and *T. aestivum*) and barley (*Hordeum vulgare* and *H. spontaneum*) (*Gramineae*). *American Journal of Botany* 86, 1615–1623.
- Bamford, M.K., Albert, R.M., Cabanes, D., 2006. Plio-Pleistocene macroplant fossil remains and phytoliths from Lowermost Bed II in the eastern palaeolake margin of Olduvai Gorge, Tanzania. *Quaternary International* 148, 95–112.
- Berlin, A.M., Ball, T., Thompson, R., Herbert, S.C., 2003. Ptolemaic agriculture, ‘Syrian wheat’, and *Triticum aestivum*. *Journal of Archaeological Science* 30, 115–121.
- Berna, F., Behar, A., Shahack-Gross, R., Berg, J., Boaretto, E., Gilboa, A., Sharon, I., Shalev, S., Shilstein, S., Yahalom-Mack, N., 2007. Sediments exposed to high temperatures: reconstructing pyrotechnological processes in Late Bronze and Iron Age Strata at Tel Dor (Israel). *Journal of Archaeological Science* 34, 358–373.
- Borowski, O., 1987. *Agriculture in Iron Age Israel*. Eisenbrauns, Winona Lake, IN.
- Brochier, J.E., Villa, P., Giacomarra, M., Tagliacozzo, A., 1992. Shepherds and sediments – geo-ethnoarchaeology of pastoral sites. *Journal of Anthropological Archaeology* 11, 47–102.
- Brown, D.A., 1984. Prospects and limits of a phytolith key for grasses in the Central United-States. *Journal of Archaeological Science* 11, 345–368.
- Bullock, P., 1985. *International Society of Soil Science, Handbook for Soil Thin Section Description*. Waine Research, Albrighton.
- Canti, M.G., 1997. An investigation of microscopic calcareous spherulites from herbivore dungs. *Journal of Archaeological Science* 24, 219–231.
- Canti, M.G., 1998. The micromorphological identification of faecal spherulites from archaeological and modern materials. *Journal of Archaeological Science* 25, 435–444.

- Canti, M.G., 1999. The production and preservation of faecal spherulites: animals, environment and taphonomy. *Journal of Archaeological Science* 26, 251–258.
- Courty, M.A., Goldberg, P., Macphail, R., 1989. *Soils and Micromorphology in Archaeology*. Cambridge University Press, Cambridge and New York.
- Elbaum, R., Weiner, S., Albert, R.M., Elbaum, M., 2003. Detection of burning of plant materials in the archaeological record by changes in the refractive indices of siliceous phytoliths. *Journal of Archaeological Science* 30, 217–226.
- Gerstel-Raban, N., Bar-Oz, G., Zohar, I., Sharon, I., Gilboa, in press. Early Iron Age Dor (Israel): A Faunal Perspective. *Bulletin of the American Schools of Oriental Research*.
- Gilboa, A., 2005. Sea Peoples and Phoenicians along the southern Phoenician Coast, a reconciliation: an interpretation of SKL material culture. *Bulletin of the American Schools of Oriental Research* 337, 47–78.
- Gilboa, A., Sharon, I., 2003. An archaeological contribution to the Early Iron Age chronological debate: alternative chronologies for Phoenicia and their effects on the Levant, Cyprus, and Greece. *Bulletin of the American Schools of Oriental Research* 332, 7–80.
- Herzog, Z., 1997. *Archaeology of the City: Urban Planning in Ancient Israel and its Social Implications*. Emery and Claire Yass Archaeology Press, Tel Aviv.
- Kamp, K., 2000. From village to tell: household ethnoarchaeology in Syria. *Near Eastern Archaeology* 63, 84–93.
- Kramer, C., 1982. *Village Ethnoarchaeology: Rural Iran in Archaeological Perspective*. Academic Press, New York.
- Macphail, R.I., Cruise, G.M., Allen, M.J., Linderholm, J., Reynolds, P., 2004. Archaeological soil and pollen analysis of experimental floor deposits; with special reference to Butser Ancient Farm, Hampshire, UK. *Journal of Archaeological Science* 31, 175–191.
- Madella, M., Alexandre, A., Ball, T., Group, I.W., 2005. International code for phytolith nomenclature 1.0. *Annals of Botany* 96, 253–260.
- Miller, N.F., 1984. The use of dung as fuel: an ethnographic example and an archaeological interpretation. *Paléorient* 10, 71–79.
- Morris, I., 1991. The early polis as city and state. In: Rich, J., Wallace-Hadrill, A. (Eds.), *City and Country in the Ancient World*. Routledge, London and New York, pp. 25–58.
- Mullholland, S.C., Rapp Jr., G., 1992. A morphological classification of grass silica-bodies. In: Rapp, G.R., Mullholland, S.C. (Eds.), *Phytolith Systematics: Emerging Issues*. Plenum Press, New York, pp. 65–89.
- Pearsall, D.M., Piperno, D.R., Dinan, E.H., Umlauf, R., Zhao, Z.J., Benfer, R.A., 1995. Distinguishing rice (*Oryza-Sativa Poaceae*) from wild *Oryza* species through phytolith analysis – results of preliminary research. *Economic Botany* 49, 183–196.
- Piperno, D.R., 2006. *Phytoliths: A Comprehensive Guide for Archaeologists and Paleoecologists*. AltaMira Press, Lanham, MD, p. 238.
- Piperno, D.R., Pearsall, D.M., 1993. Phytoliths in the reproductive structures of maize and Teosinte – implications for the study of maize evolution. *Journal of Archaeological Science* 20, 337–362.
- Reddy, S.N., 1997. If the threshing floor could talk: integration of agriculture and pastoralism during the Late Harappan in Gujarat, India. *Journal of Anthropological Archaeology* 16, 162–187.
- Reddy, S.N., 1998. Fueling the hearths in India: the role of dung in Paleoethnobotanical interpretation. *Paléorient* 24, 61–70.
- Rosen, A.M., 1992. Preliminary identification of silica skeletons from Near Eastern archaeological sites: an anatomical approach. In: Rapp, G.R., Mullholland, S.C. (Eds.), *Phytolith Systematics: Emerging Issues*. Plenum Press, New York, pp. 129–147.
- Rosen, A.M., 1993. Phytolith evidence for early cereal exploitation in the Levant. In: Pearsall, D.M., Piperno, D.R. (Eds.), *Current Research in Phytolith Analysis: Applications in Archaeology and Paleoecology*. MASCA, The University Museum of Archaeology and Anthropology, University of Pennsylvania, Philadelphia, pp. 160–171.
- Rosen, A.M., Weiner, S., 1994. Identifying ancient irrigation – a new method using opaline phytoliths from Emmer Wheat. *Journal of Archaeological Science* 21, 125–132.
- Roth, Y., 1985. *Survey of the Southern Golan*. Eretz Israel Museum Publication, Tel Aviv.
- Schiegl, S., Goldberg, P., Bar-Yosef, O., Weiner, S., 1996. Ash deposits in Hayonim and Kebara caves, Israel: macroscopic, microscopic and mineralogical observations, and their archaeological implications. *Journal of Archaeological Science* 23, 763–781.
- Shahack-Gross, R., Marshall, F., Weiner, S., 2003. Geo-ethnoarchaeology of pastoral sites: the identification of livestock enclosures in abandoned Maasai settlements. *Journal of Archaeological Science* 30, 439–459.
- Shahack-Gross, R., Marshall, F., Ryan, K., Weiner, S., 2004. Reconstruction of spatial organization in abandoned Maasai settlements: implications for site structure in the Pastoral Neolithic of East Africa. *Journal of Archaeological Science* 31, 1395–1411.
- Shahack-Gross, R., Albert, R.M., Gilboa, A., Nagar-Hilman, O., Sharon, I., Weiner, S., 2005. Geoarchaeology in an urban context: the uses of space in a Phoenician monumental building at Tel Dor (Israel). *Journal of Archaeological Science* 32, 1417–1431.
- Sharon, I., Gilboa, A., Jull, A.J.T., Boaretto, E., 2005. The Early Iron Age dating project: introduction, methodology, progress report and an update of the Tel Dor dates. In: Levy, T.E., Higham, T. (Eds.), *The Bible and Radiocarbon Dating: Archaeology, Text and Science*. Equinox Publishers, London and Oakville, CT, pp. 65–92.
- Sharon, I., Gilboa, A., in press. The SKL town: Dor in the Early Iron Age. In: Artzy, M., Killebrew, A.E. (Eds.), *Philistines and Other Sea Peoples*. Brill, Leiden.
- Tsartsidou, G., Lev-Yadun, S., Albert, R.M., Rosen, A., Efstathiou, N., Weiner, S., in press. The phytolith archaeological record: strengths and weaknesses evaluated based on a quantitative modern reference collection from Greece. *Journal of Archaeological Science*.
- Turkowski, L., 1969. Peasant agriculture in the Judean hills. *Palestine Exploration Quarterly*, 101–112.
- Twiss, P.C., Suess, E., Smith, R.M., 1969. Morphological classification of grass phytoliths. *Soil Science Society of America Proceedings* 33, 109–115.
- Watson, P.J., 1979. *Wenner-Gren Foundation for Anthropological Research, Archaeological Ethnography in Western Iran*. University of Arizona Press, Tucson, AZ.
- Whitley, J., 2001. *The Archaeology of Ancient Greece*. Cambridge University Press, New York.
- Whittaker, J.C., 2000. Alonia and Dhoukanes: the ethnoarchaeology of threshing in Cyprus. *Near Eastern Archaeology* 63, 62–69.
- Zhao, Z.J., Pearsall, D.M., Benfer, R.A., Piperno, D.R., 1998. Distinguishing rice (*Oryza sativa poaceae*) from wild *Oryza* species through phytolith analysis, II: Finalized method. *Economic Botany* 52, 134–145.
- Ziadeh-Seely, R., 1999. Abandonment and site formation processes: an ethnographic and archaeological study. In: Glock, A.E., Kapitan, T. (Eds.), *Archaeology, History and Culture in Palestine and the Near East: Essays in Memory of Albert E. Glock*. Scholars Press, Atlanta, GA, pp. 127–150.